Smoke optical properties: Lidar observations in Cyprus during 2021-2023

M. Poutli[a,c], D. Hadjimitsis[a,c], A. Nisantzi[a, c], A. Ansmann[b] and R. E. Mamouri[a, c]
[a] Eratosthenes Centre of Excellence, Limassol, 3012, Cyprus; [b]Leibniz Institute for Tropospheric Research, Leipzig, 04318, Germany; [c]Department of Civil Engineering and Geomatics, Cyprus University of Technology, Limassol, 3036, Cyprus

ABSTRACT

Climate change has affected many aspects of our lives with wildfires being one of the most important. The uncontrolled fires that occur mainly in rural or sparsely populated areas can be considered as a natural part of many ecosystems, but the changes in global climate and global warming have notably influenced their frequency and heightened risk. Smoke particles can strongly affect the climate system, by absorbing solar radiation and by influencing the evolution of clouds. Therefore, it is of great importance to investigate their optical properties. In this study we focus on the statistical analysis of smoke optical properties at different aging levels. The smoke layers were observed in the free troposphere of Limassol, Cyprus, in the summer of the period 2021-2023. Emphasis is given to the intense activity of wildfires in Turkey's Mediterranean Region in July and August 2021 as well as in the Evros region, Greece, during the summer of 2023. The analysis was performed utilizing data from the multiwavelength polarization Raman lidar, PollyXT, which is operated at the Cyprus Atmospheric Remote Sensing Observatory of the Eratosthenes Centre of Excellence at Limassol. Backward trajectories, generated with the HYSPLIT model, synergistically with VIIRS data were used to confirm the presence and the origin of smoke layers above Limassol's site. Based on the time that smoke travelled in the atmosphere above Limassol, we characterized the various cases as fresh smoke (travel time of smoke: ≤ 1day) or non-fresh smoke (travel time: ≥ 2 days). In most cases of fresh smoke layers, the particle depolarization ratio at 532 nm (7% -18%) exceeded that of non-fresh smoke (2% -10%), suggesting soil dust influence from fires or other sources. This trend was observed at both wavelengths, with 355 nm exhibiting a more complex situation. The lidar ratio values ranged approximately from 40 to 90 sr for both fresh and non-fresh cases at both wavelengths. The POLIPHON method was also applied to estimate the vertically resolved smoke mass concentration.

Keywords: wildfires, remote sensing, lidar, optical properties, POLIPHON

1. INTRODUCTION

Increased heat, prolonged drought, and reduced moisture in fuel sources such as trees and forest debris are some of the major consequences of climate change that have amplified the risk and spread of wildfires globally. According to future projections, the probability of fire incidents will be increased in many regions worldwide, including those historically less prone to fires [1]. The United States has already observed longer wildfire seasons and increased frequency [2, 3], while Southern Europe is expected to face growing wildfire risks linked to climate change [4]. Smoke particles can affect the Earth's radiation budget by absorbing solar radiation. Moreover, they can serve as cloud condensation nuclei (CCN) and ice-nucleating particles (INPs) impacting cloud formation [5, 6]. These direct and indirect effects, along with the impact of smoke on air quality and visibility, necessitate further investigation to improve our understanding of smoke optical properties. It is of great importance to further study the properties and behavior of smoke particles in different regions of the world and this work focuses on analyzing smoke optical properties above Cyprus in recent years. The geographical position of Cyprus, the easternmost part of the Eastern Mediterranean, makes it a unique point for studying aerosol mixtures from various sources, such as marine particles, desert dust from the Sahara and the Middle East, anthropogenic aerosols from urban and industrial areas in Central and Eastern Europe and North Africa, as well as smoke from biomass

Tenth International Conference on Remote Sensing and Geoinformation of the Environment (RSCy2024), edited by A. Christofe, S. Michaelides, D. Hadjimitsis, C. Danezis, K. Themistocleous, N. Kyriakides, G. Schreier, Proc. of SPIE Vol. 13212, 1321218 · © 2024 SPIE · 0277-786X · doi: 10.1117/12.3037306

burning in neighboring areas [7]. Hence, this is a great opportunity to study the behavior of smoke in such aerosol mixtures and the possible influence of other aerosol types on the optical properties.

The fire seasons during 2021-2023 had a significant impact on many regions, with southern Europe experiencing numerous extreme fire events [8]. Intense wildfire activity was observed in Turkey's Mediterranean Region during July and August 2021, resulting in the highest loss of area in the history of forest fires in Turkey [9]. More precisely, more the 200 km^2 of Coniferous Forest and 100 km^2 of Transitional woodland-shrub were burned. In addition, 20 km^2 was characterized as agricultural areas [10]. Moreover, a major wildfire occurred in the Evros region of northeastern Greece, close to the Turkish border, that started on 19 August 2023 and lasted for about 15 days, burning more than 96,000 hectares. According to the Copernicus Atmosphere Monitoring Service (CAMS) [11] this was the largest wildfire ever recorded in Europe, with the smoke plume traveling over central Greece, Crete, and southern Italy, impacting the air quality of many regions. These events, which led to tragic human losses, evacuations, and severe ecological, environmental, and economic disasters, prompted us to conduct a statistical analysis of the smoke optical properties detected in the free troposphere above Limassol.

It is well known that the depolarization ratio of smoke can vary across different altitude levels, with lower values typically observed in the lower and middle troposphere and higher values in the upper troposphere and lower stratosphere. In the former case, spherical smoke particle shapes are predominant, while in the latter case, smoke reaching these higher altitudes can display non-spherical shapes. Various factors can contribute to this phenomenon, as explained by M. Haarig et al. (2018) [12]. Our work focuses on the statistical analysis of smoke optical properties at tropospheric heights. We specifically examine changes in the lidar ratio and depolarization ratio of smoke particles at different aging levels. The polarization-lidar photometer networking (POLIPHON) method [13] is also applied to estimate the vertically resolved smoke mass concentration, as well as the potential influence of soil dust to the aerosol mixture.

2. INSTRUMENTATION

Observations were performed with a multiwavelength polarization Raman lidar, PollyXT (POrtabLe Lidar sYstem, the neXT generation) [14], which is operated at the Cyprus Atmospheric Remote Sensing Observatory (CARO) of the Eratosthenes Centre of Excellence at Limassol (34.677˚N, 33.0375˚E). It belongs to the third generation of PollyXTs systems and is housed in a container. This system runs autonomously, and it is operated 24/7 with a diode-pumped laser that emits the first (1064 nm), second (532 nm) and third (355 nm) harmonic frequency of linear polarization light with a pulse repetition rate of 100 Hz [15]. It enables the retrieval of vertically-height resolved profiles of the particle backscatter coefficient β at 355, 532 and 1064 nm, the particle extinction coefficient α at 355 and 532 nm, the corresponding extinction-to-backscatter ratios (lidar ratios, L), and the volume and particle linear depolarization ratios δ at 355 and 532 nm. The system also includes a water-vapor Raman channel (407 nm) and a second near-range receiver with four channels (355, 387, 532, and 607 nm). Now the full overlap of the overall system is at 120 m height above lidar, and more precise measurements can be made.

Figure 1. (a, b) CARO station (34.677˚N, 33.0375˚E), **(c)** Polly^{XT} lidar main subsystems.

Figure 1 (a, b) presents the CARO station with the container housing the lidar instrument, while Fig. 1c displays the main lidar subsystems. The primary subsystems of the PollyXT layout are as follows:

1. Laser source
2. Emitting optics
3. Telescope which receives the backscatter signal from the particles and molecules of the atmosphere.
4. Detection system
5. Lidar PC for the recording and storage of the data

3. DATA AND METHODOLOGY

To identify the aerosol layers in the atmosphere above Limassol, Cyprus, we utilized the information given by the plots of the temporal evolution of the attenuated backscatter signal at 1064 nm and the volume depolarization ratio at 532 nm. The presence of the smoke particles was assumed by the relatively increased backscatter coefficient values, indicating the appearance of aerosols, along with low depolarization ratios. Previous research [12], has shown that the depolarization ratio of smoke can vary across different height levels, with lower values dominating in the lower and middle troposphere. Our analysis focuses on the geometrical and optical properties of smoke particles in the free troposphere, hence our assumption of low depolarization ratio values. Backward trajectories, generated with HYSPLIT (Hybrid Single-Particle Lagrangian Integrated Trajectory model) simulations [16], synergistically with VIIRS (Visible Infrared Imaging Radiometer Suite) data [17], were used to verify the origin of the air masses and determine the altitude and the time at which the identified aerosol layers were observed above Limassol. VIIRS data are available from the joint NASA/NOAA Suomi National Polar orbiting Partnership (Suomi NPP) satellite.

The retrieval of the lidar and depolarization ratio at 355 nm and 532 nm was based on nighttime observations with a temporal average of 60-120 minutes. In most cases we selected nighttime measurements for the intervals of 20:00 and 21:00 UTC, 01:00 and 02:30 UTC, for which the Raman lidar method [18], was applied. For each case we calculated the mean values of the depolarization and lidar ratios within the detected layers and investigated their behavior and the potential differences among different aging levels of smoke.

4. RESULTS

The focus of this study is to investigate the optical properties of smoke at different aging levels upon arrival above Limassol. During the summer period spanning from 2021 to 2023, a total of 26 cases of smoke layers were analyzed. These cases were attributed to wildfire events in southern Europe and the Eastern Mediterranean, as well as local fires in the Cyprus region. In 17 out of 26 events, the smoke reached Limassol within several hours to one day after emission from the source region. These events were classified as fresh smoke cases, while the remaining 9 were categorized as non-fresh, with smoke travel times greater than or equal to 2 days.

The statistical analysis of smoke optical properties was based on nighttime observations, as detailed in the “Data and Methodology” section. Table 1 presents the mean values of the lidar ratio and particle depolarization ratio at 355 nm and 532 nm for fresh and non-fresh smoke over the entire study period. For most fresh smoke layers, the particle depolarization ratio (7% -18%) exceeded that of non-fresh smoke (2% -10%), suggesting soil dust influence from fires or other sources [7]. This trend was observed at both wavelengths, with 355 nm exhibiting a more complex behavior. The lidar ratio values ranged approximately from 40 to 90 sr for both fresh and non-fresh smoke at both wavelengths. Lidar ratio and depolarization ratio estimates found relevant to values from the literature [19, 20, 21, 22, 23].

Table 1: Mean values and standard deviations of the lidar ratio and particle depolarization ratio at 355 nm and 532 nm. These values were estimated based on smoke layers that were observed at the atmosphere of Limassol during the summer period from 2021 to 2023.

	532 nm		355 nm	
	Fresh smoke [17 cases]	**Non-fresh smoke [9 cases]**	**Fresh smoke [17 cases]**	**Non-fresh smoke [9 cases]**
Lidar ratio (sr)	51.16 ± 8.57	54.80 ± 13.03	63.85 ± 13.49	58.10 ± 13.50
Part. depol. ratio (%)	11.16 ± 3.66	6.38 ± 3.22	7.52 ± 2.87	4.69 ± 1.83

In the following subsections, we present two case studies that are representative of fresh and non-fresh smoke events. On July 30, 2021, an intense smoke plume was advected from wildfires in Turkey and reached Limassol after a few hours, affecting the structure of the atmosphere. This event was categorized as fresh smoke. Conversely, on July 1, 2023, Limassol experienced the presence of non-fresh smoke particles, traced back to a dispersed plume originating near Italy and Portugal on June 28.

4.1 Fresh smoke: The case of 30th of July 2021

According to World Meteorological Organization (WMO), extreme temperatures were observed across the Mediterranean Basin during 2021. Turkey's Mediterranean coasts were particularly affected by these extreme events, influenced by both global climate change and the characteristic features of the Mediterranean climate. Data from the Republic of Turkey Ministry of Agriculture and Forestry indicate that extensive wildfires occurred throughout a large part of Turkey in August 2021. The wildfire event started on 28 July 2021 and lasted for about 15 days causing significant damage to large areas and reaching the level of disaster [9].

On the 30th of July 2021, in the early morning, the PollyXT instrument detected an intense particle layer that reached 3 km height. According to HYSPLIT trajectories, these particles originated from the wildfires in Turkey's Mediterranean Region that started on 28th of July. In Figure 2a, the backward trajectories generated using GDAS meteorological data confirmed the passage of air masses from the burning areas a few hours after the onset of the event. The VIIRS on the Suomi NPP satellite captured a significant smoke plume on 29th of July (Fig. 2b), which then dispersed, affecting the atmosphere of Cyprus (Fig. 2c, d). This ascertains the presence of smoke particles in the area under study.

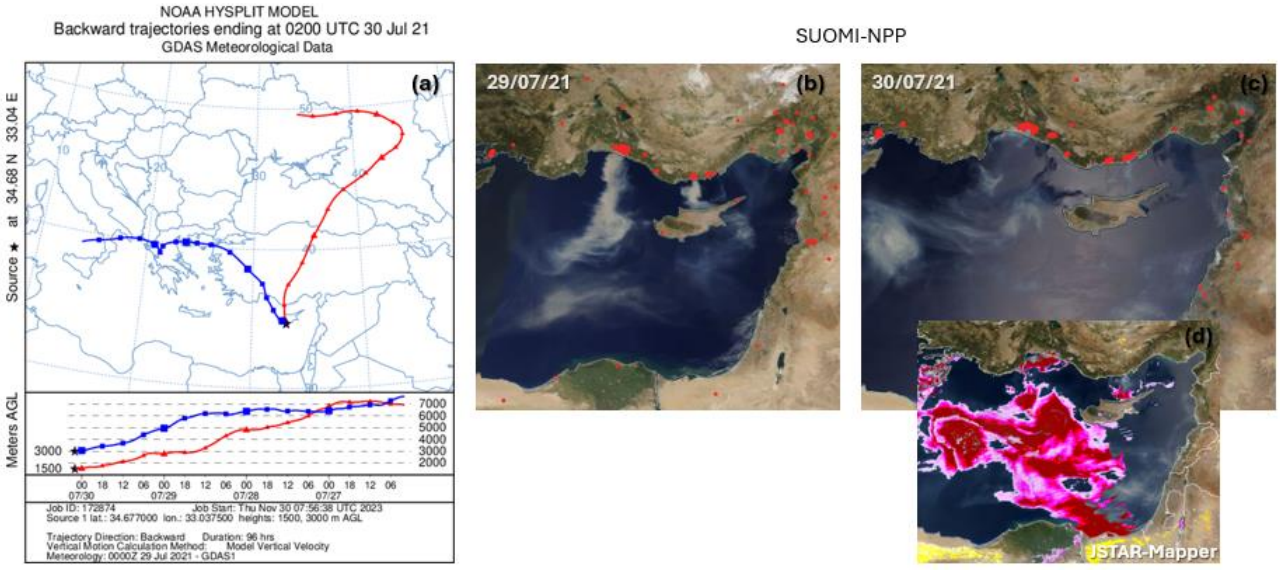

Figure 2. (a) HYSPLIT 4-d trajectories arriving at 1500m and 3000m over Limassol, Cyprus, on 30 July 2021, 02:00 UTC, **(b), (c)** true-color images captured by VIIRS on board Suomi NPP during 29-30 July 2021 (source: NASA Worldview, https://worldview.earthdata.nasa.gov/), **(d)** Aerosol Index captured by VIIRS, purple color indicates the presence of smoke particles (source: NOAA JSTAR-Mapper, https://www.star.nesdis.noaa.gov/mapper/).

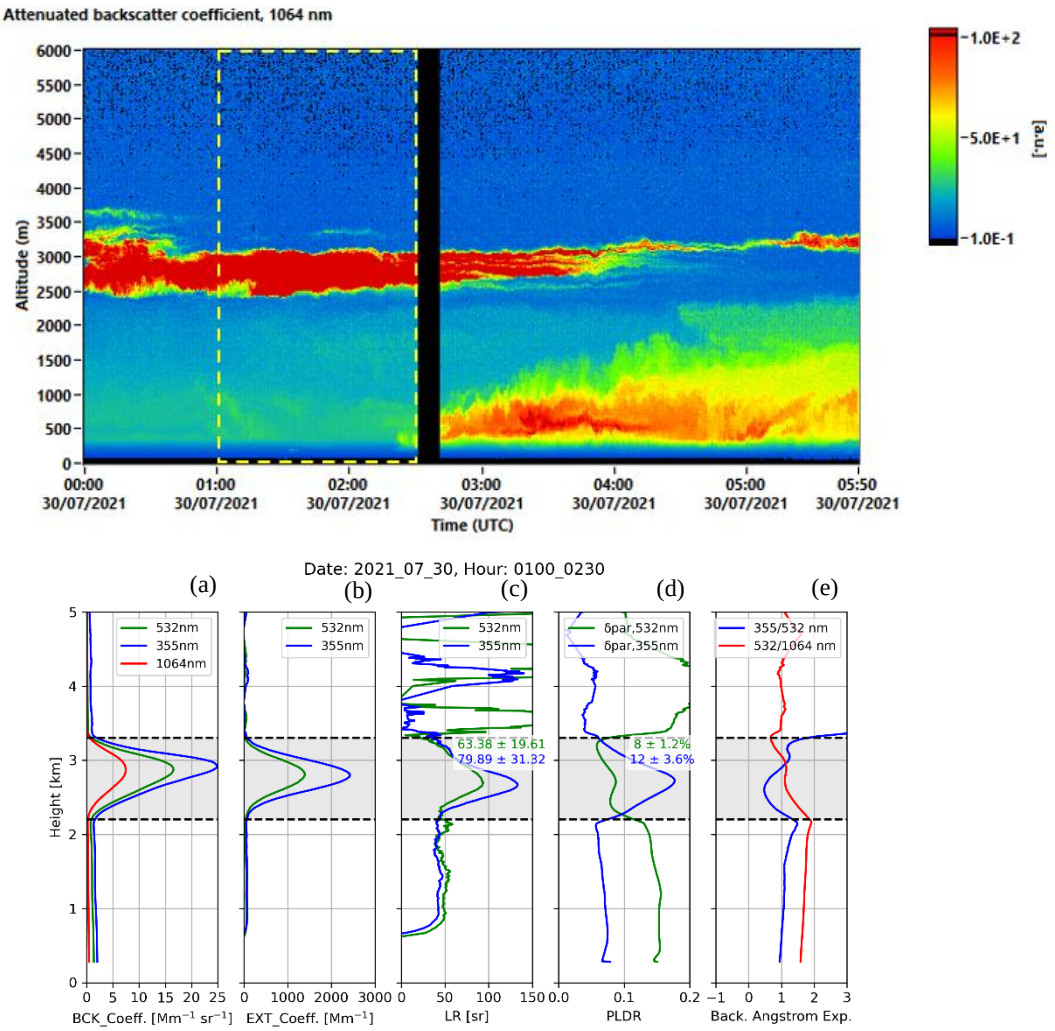

Figure 3. (top) Temporal evolution of the attenuated backscatter coefficient at 1064 nm from the PollyXT lidar system on 30/07/2021, 00:00-05:50 UTC, and **(bottom)** (a) vertical profiles of the particle backscatter coefficients at 355, 532, 1064 nm, (b) extinction coefficient at 355, 532 nm, (c) lidar ratios at 355 and 532 nm, (d) particle linear depolarization ratios at 355 and 532 nm, and (e) backscatter-related Ångström exponents (red: 532–1064 nm spectrum, and blue: 355-532 nm).

Figure 3 (top) presents the temporal evolution of the attenuated backscatter coefficient at 1064 nm between 00:00 and 05:50 UTC on 30 July 2021, as measured by the PollyXT instrument. The presence of an intense aerosol structure can be seen clearly from 00:00 UTC at approximately 2.5-3.0 km height. To estimate the mean values of the lidar ratio and the particle depolarization ratio in the detected layer, the lidar signal was averaged in a 1.30-h time-window (yellow dashed-box, 01:00-02:30 UTC). In Figure 3 (bottom) the vertical profiles of the backscatter and extinction coefficients, the lidar and depolarization ratios and the backscatter-related Ångström exponents on July 30, 2021, are also presented. The increased values of the particle backscatter coefficient in Fig. 3a (bottom) indicated a significant presence of aerosols at the height range of 2.2-3.4 km. More precisely, the maximum value of the backscatter coefficient at 355 nm was 24.90 Mm^{-1} sr^{-1}, while 16.56 and 7.47 Mm^{-1} sr^{-1} at 532 and 1064 nm, respectively. The extinction coefficient (Fig.3b, bottom) displayed extreme values at both wavelengths with 1397.60 Mm^{-1} at 532 nm and 2429.02 Mm^{-1} at 355 nm. The backscatter-related Ångström exponents (Fig. 3e, bottom) averaged close to 1 indicating the presence of fine-mode particles [15], a characteristic of smoke. The 355 nm mean lidar ratio and depolarization ratio for the fresh smoke (2.2-3.4 km) were found to be 79.89 ± 31.32 sr and 12 ± 3.6 %, respectively. The respective values at 532 nm were equal to 63.38 ± 19.61 sr and 8

± 1.2 %. The ratio of lidar ratios (LR532/LR355) was less than 1 for fresh particles, which is in good agreement with the literature [12, 21, 22]. The slightly enhanced values of the particle depolarization ratio suggested the presence of almost spherical particles, indicating the possible influence of soil dust and dust injected during the fire in the aerosol mixture [7].

The polarization-lidar photometer networking (POLIPHON) method was applied for the height-resolved separation of smoke and dust aerosol backscatter and extinction, and mass concentration at 532 nm, to investigate the presence of dust during the fresh smoke event that occurred on 30/07/21. The detailed procedure for the one-step POLIPHON method used is well described by R.E. Mamouri and A. Ansmann (2014) [13]. To distinguish smoke and dust particles in terms of particle backscatter coefficient, we employed depolarization ratios of 0.31 for dust and 0.05 for smoke (non-dust). To estimate the vertically resolved mass concentration, we first determined the extinction coefficient profiles. For smoke particles we used a lidar ratio equal to the respective mean value in the detected layer of smoke, while for dust particles, we applied a lidar ratio of 50 sr according to the literature. To calculate the mass concentration, we used particle densities of 2.6 g cm^{-3} for dust particles and 1.2 g cm^{-3} for smoke particles, following the findings from reported studies [13, 24]. The required particle volume-to-extinction conversion factors used were 0.16×10^{-6} m, 0.3×10^{-6} m, and 0.8×10^{-6} m for fine-mode spherical particles (smoke in this case), fine dust, and coarse dust, respectively [13, 24]. Fine mode non-dust particles dominated the particle layer at 2.2-3.4 km, with backscatter and extinction coefficients reaching maximum values equal to 18.72 Mm^{-1} sr^{-1} and 1314.08 Mm^{-1}, respectively (Fig. 4, left and middle panels). While fine and coarse dust particles were also present, their contribution to height profiles of backscatter and extinction coefficients appeared significantly smaller. In terms of particle mass concentration, the dust contribution in the mixed aerosol plume was higher. Coarse dust particles and non-dust particles displayed mass concentrations with maximum values approximately of 300 µg m^{-3}, while fine dust showed values up to 50 µg m^{-3} for the smoke case observed on 30 July 2021. Hence, the influence of some irregularly shaped soil dust particles on the slightly enhanced depolarization ratios (Fig. 3d, bottom) was confirmed.

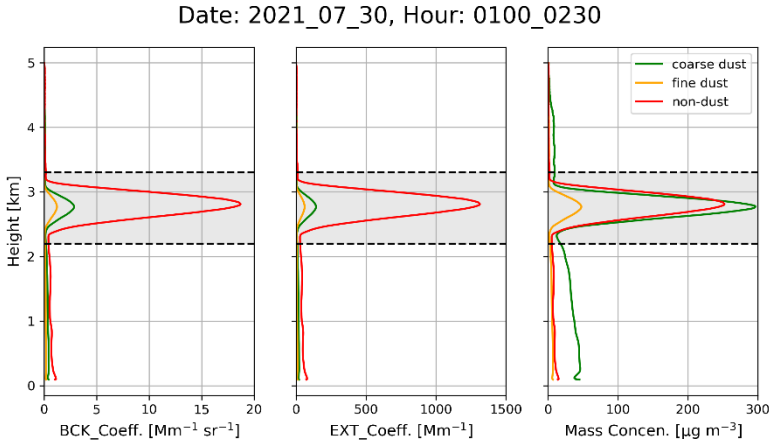

Figure 4. Results from the one-step POLIPHON method: **(a)** 532 nm particle backscatter coefficient vertical profiles for coarse-mode dust particles (green curve), fine-mode dust particles (orange curve) and fine-mode non-dust particles (red curve), **(b)** particle extinction coefficient profiles for the same aerosol types and, **(c)** particle mass concentration profiles. Mass concentrations were determined from the extinction coefficient profiles after R. E. Mamouri and A. Ansmann (2014). The profiles refer to measurements on 30 July, during the same 1.30-hour time window (01:00-02:30 UTC) in which the lidar signal was averaged to estimate the mean values of the optical properties.

4.2 Non-fresh smoke: The case of 1st of July 2023

On the 1st of July 2023 an intense aerosol layer was observed by the PollyXT lidar system at Limassol's site at noon, in the height range of 1.0-3.0 km. According to HYSPLIT simulations, the air masses, transferred smoke particles from a dispersed plume detected near the regions of Italy and Portugal on the 28th of June, to the atmosphere of Cyprus four days later. The profiles of the optical properties and the mean values of the lidar ratio and the particle depolarization ratio indicated the presence of smoke in Limassol's atmosphere. Nevertheless, due to the dispersion area of the smoke plume and the air masses pathways reaching Limassol, the potential impact of other aerosol types contribution in the aerosol mixture cannot be excluded.

Figure 5a presents the backward trajectories of the air masses that crossed the area where the dispersed smoke plume was detected by VIIRS (Fig. 5b). According to these trajectories, the smoke particles were transported to the atmosphere over Cyprus four days after the event was noticed. In Fig. 5b the smoke plume, possibly originating from wildfires in Italy and Portugal, can be seen clearly, while Fig. 5c presents the aerosol index of smoke (purple) confirming the presence of this aerosol type. The temporal evolution of the backscatter coefficient at 1064 nm (Fig. 6, top) shows the presence of an aerosol layer on 1 July 2023 afternoon at approximately 1.0-3.0 km. To obtain the profile of the lidar ratio and investigate its behavior, we chose nighttime measurements and the lidar signal was averaged in a 1-h time-window (yellow dashed-box, 20:00-20:59 UTC). The vertical profiles of the optical properties are presented in Fig. 6 (bottom), where the detected layer is shaded with a light gray color. The backscatter coefficient (Fig. 6a) showed maximum value of 3.38 Mm^{-1} sr^{-1} at 355 nm, 1.45 Mm^{-1} sr^{-1} at 532 nm and 0.55 Mm^{-1} sr^{-1}. The extinction coefficient (Fig. 6b) reached values close to 120 Mm^{-1} at 355 nm, while at 532 nm the maximum value was approximately 80 Mm^{-1}. The backscatter-related Ångström exponent values (Fig. 6e) ranged between 1 and 2, indicating the presence of fine-mode particles. The mean lidar ratio and depolarization ratio (Fig. 6c, d, respectively) within the detected aerosol layer were found to be 39.71 ± 8.74 sr and 4 ± 0.5 % at 355 nm, respectively. The respective values at 532 nm were equal to 59.39 ± 12.28 sr and 4 ± 0. 4 %. At this case, the higher value of the lidar ratio at 532 nm was indicative of the presence of non-fresh smoke [12, 21, 22]. These estimates are relevant to literature findings [19, 20, 21, 22, 23] and alongside the values of the backscatter-related Ångström exponents indicate the presence of non-fresh smoke particles in the aerosol mixture.

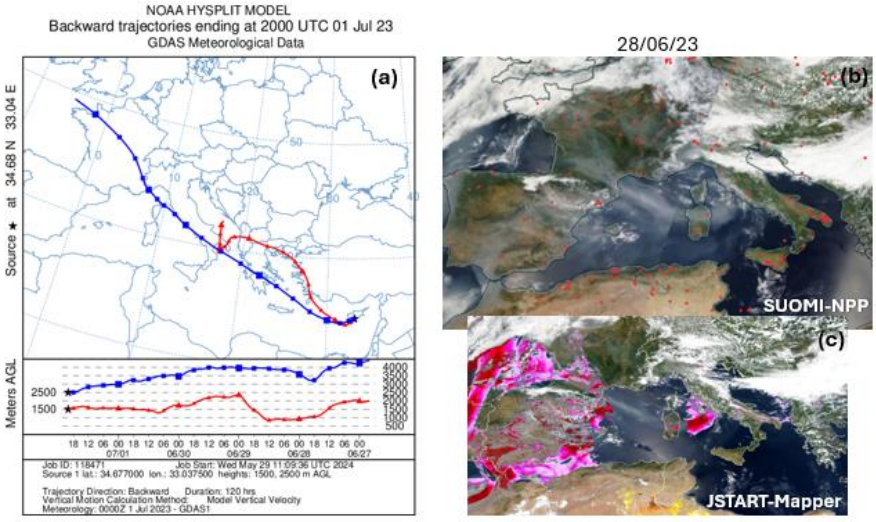

Figure 5. (a) HYSPLIT 5-d trajectories arriving at 1500m and 2500m over Limassol, Cyprus, on 1 July 2023, 20:00 UTC, **(b)** true-color images captured by VIIRS on board Suomi NPP on 28 June 2023 (source: NASA Worldview, https://worldview.earthdata.nasa.gov/), **(c)** Aerosol Index captured by VIIRS, purple color indicates the presence of smoke particles, (source: NOAA JSTAR-Mapper, https://www.star.nesdis.noaa.gov/mapper/).

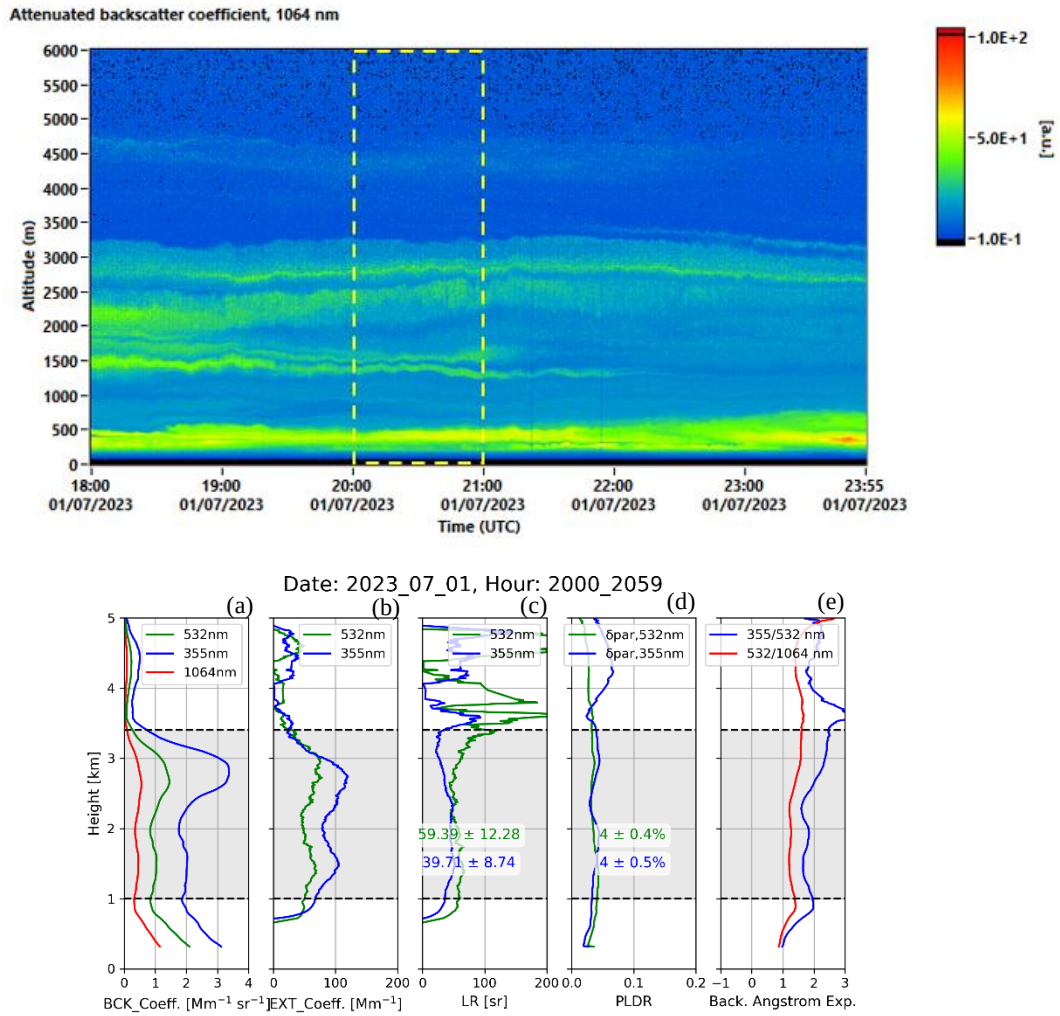

Figure 6. Same as Fig. 3 except for the datetime. Here the measurements are presented for 01/07/2023, **(top)** 18:00-23:55 UTC, and **(bottom)** 20:00-20:59 UTC.

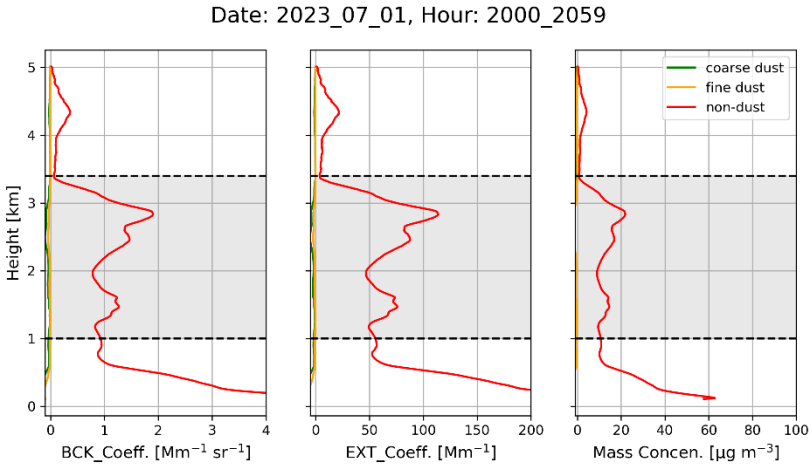

Figure 7. Same as Fig. 4 apart from the datetime. Here the POLIPHON method was applied for the PollyXT measurements on 01/07/2023 during 20:00-20:59 UTC.

In this case of non-fresh smoke, the POLIPHON method indicated that dust particles did not contribute to the composition of the layer at 1.0-3.3 km. The backscatter and extinction coefficients of fine and coarse dust showed zero values, while the corresponding values for non-dust aerosols reached values close to 2 Mm^{-1} sr^{-1} and 115 Mm^{-1}. In the height profile particle mass concentration, only the non-dust particles played a significant role, with maximum value equal to 21.85 μg m^{-3}.

5. CONCLUSIONS

In this study a total of 26 smoke cases were analyzed with 17 classified as fresh smoke cases (travel time of smoke: ≤ 1 day), and the remaining 9 categorized as non-fresh (travel time: ≥ 2 days). Observations of slightly enhanced values of the depolarization ratio at both wavelengths in most cases of fresh smoke layers suggested an influence of soil dust from fires or other sources. The two case studies presented here indicated this trend and confirmed the possible contribution of dust particles in the aerosol mixture when the plume reaches the area under study within less than 1 day after the emission of the smoke. The lidar ratio displayed almost the same range of values at both wavelengths with these estimates being consistent with those reported in recent studies. It should be noted that the behavior of the lidar ratio for fresh smoke particles at the two wavelengths, with 355 nm values being greater than or equal to 532 nm lidar ratio values, was not observed in every case. Similarly, for non-fresh smoke, the literature suggests that the LR532/LR355 ratio is greater than 1, which was not consistently observed in our study. Our study can be considered a preliminary step in understanding the optical properties of smoke in the Cyprus region, and further research is required to support and explain our findings.

ACKNOWLEDGEMENTS

The authors acknowledge the 'EXCELSIOR': ERATOSTHENES: EXcellence Research Centre for Earth Surveillance and Space-Based Monitoring of the Environment H2020 Widespread Teaming project (www.excelsior2020.eu). The 'EXCELSIOR' project has received funding from the European Union's Horizon 2020 research and innovation programme under Grant Agreement No 857510, from the Government of the Republic of Cyprus through the Directorate General for the European Programmes, Coordination and Development and the Cyprus University of Technology. The study is supported as well by the ACCEPT project (prot. no. LOCALDEV0008) co-financed by the Financial Mechanism of Norway (85 %) and the Republic of Cyprus (15 %) in the framework of the programming period 2014–2021.

REFERENCES

[1] V. Masson-Delmotte et al., "IPCC, 2021: Summary for Policymakers" in Climate Change 2021, The Physical Science Basis, Contribution of Working Group I to the Sixth Assessment Report of the Intergovernmental Panel on Climate Change, ed. (Cambridge University Press, Cambridge, United Kingdom and New York, USA 2021).

[2] Markon, C., Gray, S., Berman, M., L. Eerkes-Medrano, Hennessy, T., Huntington, H., Littell, J., McCammon, M., Thoman, R. and S. Trainor "Impacts, Risks, and Adaptation in the United States: Fourth National Climate Assessment, Volume II: Report-in-Brief," Fourth National Climate Assessment II, 1185–1241 (2018). https://nca2018.globalchange.gov/chapter/26/%0Ahttps://nca2018.globalchange.gov/downloads/NCA4_Ch26_Alaska_Full.pdf.

[3] Westerling, A.L., "Increasing western U.S. forest wildfire activity: Sensitivity to changes in the timing of spring," Phil. Trans. R. Soc. B., 371:20150178 (2016). https://doi.org/10.1098/rstb.2015.0178

[4] Dupuy, J. luc, Fargeon, H., Martin-StPaul, N., Pimont, F., Ruffault, J., Guijarro, M., Hernando, C., Madrigal, J. and Fernandes, P., "Climate Change Impact on Future Wildfire Danger and Activity in Southern Europe: A Review", Ann. For. Sci. 77 (35), (2020). https://doi.org/10.1007/s13595-020-00933-5

[5] Engel, I., Luo, B.P., Pitts, M.C., Poole, L.R., Hoyle, C.R., Grooß, J.U., Dörnbrack, A. and Peter, T., "Heterogeneous formation of polar stratospheric clouds-Part 2: Nucleation of ice on synoptic scales," Atmos. Chem. Phys. 13 (21), 10769–10785 (2013). https://doi.org/10.5194/acp-13-10769-2013

[6] Knopf, D. A., Alpert, P. A. and Wang, B, "The Role of Organic Aerosol in Atmospheric Ice Nucleation: A Review," ACS Earth and Space Chem. 2, 168-202 (2018). https://doi.org/10.1021/acsearthspacechem.7b00120

[7] Nisantzi, A., Mamouri, R., Ansmann, A. and Hadjimitsis, D., "Injection of mineral dust into the free troposphere during fire events observed with polarization lidar at Limassol, Cyprus." Atmos. Chem. Phys. 14(22), 12155-12165 (2014). https://doi.org/10.5194/acp-14-12155-2014

[8] Miller, J., Böhnisch, A., Ludwig, R. and Brunner, M. I., "Climate change impacts on regional fire weather in heterogeneous landscapes of central Europe," Nat. Hazards Earth Syst. Sci. 24(2), 411-428 (2024). https://doi.org/10.5194/nhess-24-411-2024

[9] Acar, Z. and Gonencgil, B., "Forest fires in southern Turkey July-August 2021," Revista de Climatología 23, 46–57 (2023). https://doi.org/10.59427/rcli/2023/v23.46-57

[10] Mamouri, R.-E., Ene, D., Baars, H., Engelmann, R., Nisantzi, A., Prodromou, M., Hadjimitsis, D. and Ansmann, A., "Investigation of 2021 summer wildfires in the Eastern Mediterranean: The ERATOSTHENES Centre of Excellence capabilities for atmospheric studies," EGU General Assembly 2023, Vienna, Austria, EGU23-12585. https://doi.org/10.5194/egusphere-egu23-12585

[11] CAMS (Copernicus Atmosphere Monitoring Service): https://atmosphere.copernicus.eu/

[12] Haarig, M., Ansmann, A., Baars, H., Jimenez, C., Veselovskii, I., Engelmann, R. and Althausen, D., "Depolarization and lidar ratios at 355, 532, and 1064 nm and microphysical properties of aged tropospheric and stratospheric Canadian wildfire smoke," Atmos. Chem. Phys. 18(16), 11847–11861 (2018). https://doi.org/10.5194/acp-18-11847-2018

[13] Mamouri, R. E. and Ansmann, A., "Fine and coarse dust separation with polarization lidar," Atmospheric Measurement Techniques 7(11), 3717–3735 (2014). https://doi.org/10.5194/amt-7-3717-2014

[14] Engelmann, R., Kanitz, T., Baars, H., Heese, B., Althausen, D., Skupin, A., Wandinger, U., Komppula, M., Stachlewska, I.S., Amiridis, V., Marinou, E., Mattis, I., Linne, H. and Ansmann, A., "The automated multiwavelength Raman polarization and water-vapor lidar PollyXT: The neXT generation," Atmospheric Measurement Techniques 9(4), 1767–1784 (2016). https://doi.org/10.5194/amt-9-1767-2016

[15] Mamouri, R.E., Ansmann, A., Ohneiser, K., Knopf, D.A., Nisantzi, A., Bühl, J., Engelmann, R., Skupin, A., Seifert, P., Baars, H., Ene D., Wandiger, U. and Hadjimitsis, D. "Wildfire smoke triggers cirrus formation: lidar observations over the eastern Mediterranean", Atmos. Chem. Phys 23(22), 14097–14114 (2023). https://doi.org/10.5194/acp-23-14097-2023

[16] HYbrid Single-Particle Lagrangian Integrated Trajectory model, backward trajectory calculation tool, National Oceanic and Atmospheric Administration (NOAA), https://www.ready.noaa.gov/HYSPLIT.php.

[17] FIRMS (Fire Information for Resource Management System): https://firms.modaps.eosdis.nasa.gov/.

[18] Ansmann, A., Wandinger, U., Riebesell, M., Weitkamp, C. and Michaelis, W., "Independent measurement of extinction and backscatter profiles in cirrus clouds by using a combined Raman elastic–backscatter lidar," Applied Optics 31(33), 7113–7131 (1992). https://doi.org/10.1364/AO.31.007113

[19] Floutsi, A.A., Baars, H., Engelmann, R., Althausen, D., Ansmann, A., Bohlmann, S., Heese, B., Hofer, J., Kanitz, T., Haarig, M., et al., "DeLiAn - a growing collection of depolarization ratio, lidar ratio and Ångström exponent for different aerosol types and mixtures from ground-based lidar observations," Atmospheric Measurement Techniques 16(9), 2353–2379 (2023). https://doi.org/10.5194/amt-16-2353-2023

[20] Mylonaki, M., Papayannis, A., Anagnou, D., Veselovskii, I., Papanikolaou, C.A., Kokkalis, P., Soupiona, O., Foskinis, R., Gidarakou, M. and Kralli, E., "Optical and microphysical properties of aged biomass burning aerosols and mixtures, based on 9-year multiwavelength raman lidar observations in athens, Greece," Remote Sensing 13(19), (2021). doi:10.3390/rs13193877

[21] Adam, M., Nicolae, D., Stachlewska, I.S., Papayannis, A., and Balis, D., "Biomass burning events measured by lidars in EARLINET – Part 1: Data analysis methodology," Atmospheric Chemistry and Physics 20(22), 13905–13927 (2020). https://doi.org/10.5194/acp-20-13905-2020

[22] Nicolae, D., Nemuc, A., Müller, D., Talianu, C., Vasilescu, J., Belegante, L., and Kolgotin, A., "Characterization of fresh and aged biomass burning events using multiwavelength Raman lidar and mass spectrometry," Journal of Geophysical Research Atmospheres 118(7), 2956–2965 (2013). https://doi.org/10.1002/jgrd.50324

[23] Balis, D.S., Amiridis, V., Zerefos, C., Gerasopoulos, E., Andreae, M., Zanis, P., Kazantzidis, A., Kazadzis, S., and Papayannis, A., "Raman lidar and sunphotometric measurements of aerosol optical properties over Thessaloniki, Greece during a biomass burning episode," Atmospheric Environment 37(32), 4529–4538 (2003). https://doi.org/10.1016/S1352-2310(03)00581-8

[24] Ansmann, A., Ohneiser, K., Mamouri, R.E., Knopf, D.A., Veselovskii, I., Baars, H., Engelmann, R., Foth, A., Jimenez, C., Seifert, P., et al., "Tropospheric and stratospheric wildfire smoke profiling with lidar: Mass, surface area, CCN, and INP retrieval," Atmospheric Chemistry and Physics 21(12), 9779–9807 (2021). https://doi.org/10.5194/acp-21-9779-2021